ФИЗИКА ЭЛЕМЕНТАРНЫХ ЧАСТИЦ И АТОМНОГО ЯДРА
2010. Т. 41. ВЫП. 7

ENERGY DISTRIBUTIONS OF FIELD EMITTED ELECTRONS FROM FEW-LAYER GRAPHENE SHEETS WITH AB AND ABC STACKING

V. L. Katkov, V. A. Osipov

Joint Institute for Nuclear Research, Dubna

We study the effect of the band structure on the energy distributions of field emitted electrons from AB and ABC graphene multilayers. The characteristic subpeaks are found to appear for each type of stacking. The experimental discovery of these peaks in field emission experiments from carbon few-layer systems can provide important information about the type of stacking.

PACS: 11.10.-z

INTRODUCTION

Recently, free-standing carbon nanosheets (CNSs) have been synthesized on a variety of substrates by radio frequency plasma enhanced chemical vapor deposition [1, 2]. The sheets consist of several graphene layers and stand roughly vertical to the substrate. It has been found that CNSs have good field emission characteristics with promising applications in vacuum microelectronic devices [3–6]. High emission total current at low threshold field enables using CNSs as an effective cold cathode material.

There are two known forms of bulk graphite called as AB (Bernal) and ABC (rhombohedral) with different stacking of layers. The AB phase is thermodynamically stable and this form of graphite occurs naturally. At the same time, the ABC form was also experimentally observed [7]. Thus, generally the CNSs synthesized by radio frequency plasma enhanced chemical vapor deposition can have both types of stacking.

Until now, only the current-voltage characterization was used in studies of CNSs. At the same time, voltage dependent field emission energy distribution (V-FEED) analysis is known as a powerful experimental method to interrogate the field emission. As compared to classical I–V characterization, V-FEED analysis can provide more information related to both inherent properties of the emitter and to the basic tunneling process [8]. In particular, in single-walled carbon nanotubes (CNTs), the FEED has shown characteristic peaks originated from

the stationary waves in the cylindrical part of the nanotube [9]. Their number and sharpness were found to increase with the length of the tubes. Notice that short periodic variations were also observed in the thickness-dependent field emission current from ultrathin metal films (UMF) [10]. The calculated electron energy distribution curve characteristic of UMF was found to have «steps» which correspond with the quantized «normal» energies [11]. The resonant-tunneling peaks with specific microscopic tunneling mechanisms were also observed in field emission from nanostructured semiconductor cathodes [12]. A different example of the quantum size effect in CNTs, which originates from the intrinsic properties of the energy band structure, was revealed in field emission [13]. It is reasonable to expect manifestation of quantum size effects in subnanometer CNSs. Notice that the FEED for few-Bernal-stacking layers was studied in [14].

In this paper, we calculate the FEED of electrons from three (ABC)- and four (ABCA)-layered graphene structures. The energy band structure of few-layer carbon systems resulting from the tight-binding approach is accounted for. FEEDs are calculated by using the independent channel method suggested recently in [15]. We found that the FEED experiments can give information about the type of stacking in few-layer graphene as well as provide direct verification of the high sensitivity of the band structure to the number of layers in few-layer graphene reported recently in [16].

1. BAND STRUCTURE OF AB MULTILAYERS

The band structure of graphene multilayers has been obtained within the tight-binding approach in [17]. Besides, an approximation to the dispersion relation can be found from Slonzewski–Weiss–McClure (SWMcC) model for graphite with Bernal stacking [18, 19]. SWMcC model describes the wave-vector dependence of electron energy in the vicinity of the HKH edge of the Brillouin zone. The electron energy spectrum is obtained from the equation

$$\det |H - \varepsilon| = 0, \tag{1}$$

where

$$H = \begin{pmatrix} E_1 & 0 & H_{13} & H_{13}^* \\ 0 & E_2 & H_{23} & -H_{23}^* \\ H_{13}^* & H_{23}^* & E_3 & H_{33} \\ H_{13} & -H_{23} & H_{33}^* & E_3 \end{pmatrix} \tag{2}$$

and

$$
\begin{aligned}
E_1 &= \Delta + \gamma_1\Gamma + \frac{1}{2}\gamma_5\Gamma^2, \\
E_2 &= \Delta - \gamma_1\Gamma + \frac{1}{2}\gamma_5\Gamma^2, \quad E_3 = \frac{1}{2}\gamma_2\Gamma^2, \\
H_{13} &= \frac{1}{\sqrt{2}}(-\gamma_0 + \gamma_4\Gamma)\exp(i\alpha)\sigma, \\
H_{23} &= \frac{1}{\sqrt{2}}(\gamma_0 + \gamma_4\Gamma)\exp(i\alpha)\sigma, \quad H_{33} = \gamma_3\Gamma\exp(i\alpha)\sigma
\end{aligned}
\tag{3}
$$

with $\Gamma = 2\cos(k_\perp c)$, $\sigma = k_{||}\sqrt{3}/2a = p_{||}v_F/\gamma_1$, $k_\perp$ being the wavevector projection onto the direction HKH, $k_{||}$ — the modulus of the wavevector in the yz-plain (see Fig. 1), α — the angle between $\mathbf{k}_{||}$ and the direction ΓK, c — the distance between the nearest neighbour layers, a — the lattice constant, $\mathbf{p}_{||}$ — the momentum in the yz-plain, and v_F — the Fermi velocity. Parameters γ_i describe interactions between atoms and Δ is the energy difference between two sublattices in each graphene layer. In [20], graphite parameters were estimated as $\gamma_0 = 3.16$ eV, $\gamma_1 = 0.39$ eV, $\gamma_2 = -0.020$ eV, $\gamma_3 = 0.315$ eV, $\gamma_4 = -0.044$ eV, $\gamma_5 = 0.038$ eV, and $\Delta = -0.008$ eV. The spectrum of few-layer graphene can be obtained from Eq. (1) by replacing Γ by

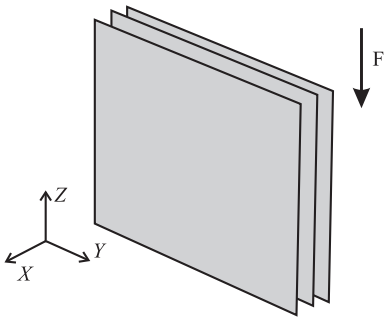

Fig. 1. The location of a graphene sheet with respect to the electric field

$$
\Gamma^n = 2\cos\left(\frac{\pi n}{N+1}\right), \quad n = 1\ldots N, \tag{4}
$$

where N is the number of layers. For graphene bilayer $N = 2$ and $\gamma_2 = \gamma_5 = 0$, so that Eq. (1) with account taken of Eq. (4) gives the result of [21] while for $N = 1$ (only γ_0 differs from zero) it reproduces the known tight-binding spectrum of graphene.

As a first approximation one can neglect all interactions except between the nearest-neighbor atoms in the same layer and between A-type atoms between adjacent layers (which are on the top of each other), i.e., all parameters except for γ_0 and γ_1 are put to be zero. Then the spectra of multilayers can be approximated by

$$
\varepsilon^n_{c,v} = \pm\left(\sqrt{\left(\frac{\gamma_1^n}{2}\right)^2 + p_{||}^2 v_F^2} - \frac{\gamma_1^n}{2}\right), \tag{5}
$$

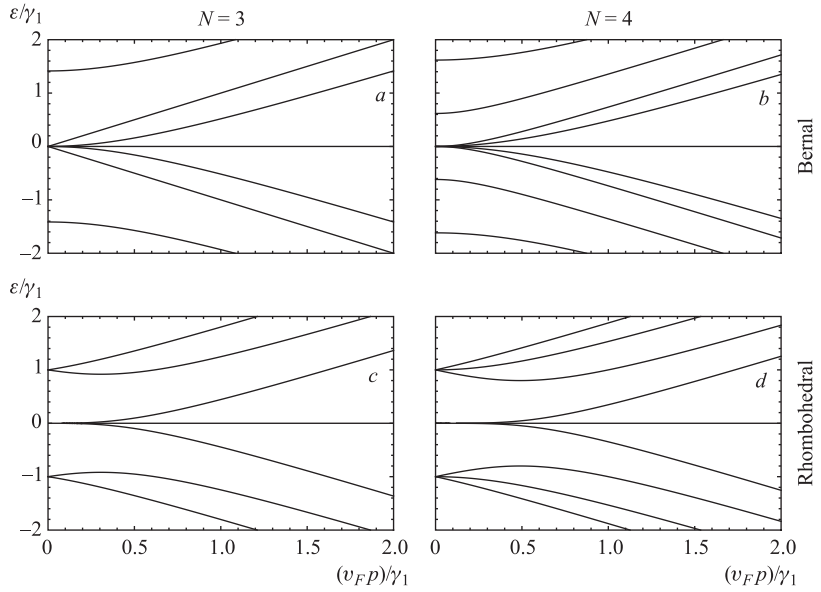

Fig. 2. Low-energy bands for ABA, ABAB and ABC, ABCA graphene multilayers

where $\gamma_1^n = \gamma_1 \Gamma^n$. The spectrum of ABA and ABAB structures calculated by using of (5) is shown in Fig. 2.

2. BAND STRUCTURE OF ABC MULTILAYERS

We assume that only $\gamma_0, \gamma_1 \neq 0$ and use the same notation as in ABA graphite, for the nearest intralayer and interlayer coupling, respectively. Although the band parameters are not identical between ABA and ABC graphites, we refer to the values of ABA in the following calculations, assuming that the corresponding coupling parameters have similar values [22].

The spectrum is obtained from (1) with Hamiltonian [22–24]

$$H_{\mathrm{ABC}} = \begin{pmatrix} H & V & & & \\ V^\dagger & H & V & & \\ & V^\dagger & H & V & \\ & & \ddots & \ddots & \ddots \end{pmatrix}, \tag{6}$$

where

$$H = \begin{pmatrix} 0 & \upsilon_F p_- \\ \upsilon_F p_+ & 0 \end{pmatrix}, \quad V = \begin{pmatrix} 0 & 0 \\ \gamma_1 & 0 \end{pmatrix}, \tag{7}$$

and $p_\pm = p_y \pm i p_z$. The number of columns and rows of matrix (6) is equal to a half number of layers $N/2$. The band structure of ABC and ABCA graphene is shown in Fig. 2.

3. FEED CALCULATION

Let us consider the graphene layer in the presence of the external electric field F directed along the z axis (see Fig. 1). The emitted current density takes the following form:

$$j^{\text{out}} = \frac{2e}{h^3} \int dp_x \int dp_y \int f(\varepsilon)\, \upsilon_g D(\varepsilon, p_x, p_y)\, dp_z, \tag{8}$$

where e is the electric charge; $h = 2\pi\hbar$ — the Planck constant; ε — the energy; $\mathbf{p}$ — momentum; $f(\varepsilon) = [\exp(\varepsilon/kT) + 1]^{-1}$ — the Fermi–Dirac distribution function; $D(\varepsilon, p_x, p_y)$ — the transmission probability of an electron through a potential barrier, and $\upsilon_g = \partial\varepsilon/\partial p_z$ — the group velocity. The integrals are over the first Brillouin zone with account taken of the positivity of υ_g.

For a two-dimensional (2D) structure, one can use the relation $\int f(p_x) dp_x = f(0)h/l_x$. Moreover, when a graphene sheet has the finite size in the y-direction, p_y is quantized. Therefore, the current density in Eq. (8) can be written as

$$j^{\text{out}} = \frac{2e}{h l_x l_y} \sum_q \int\limits_{\varepsilon^q_{\min}}^{\varepsilon^q_{\max}} f(\varepsilon^q) D(\varepsilon^q)\, d\varepsilon^q, \tag{9}$$

where the Fermi energy is chosen to be zero. Limits $\varepsilon^q_{\max}$ and $\varepsilon^q_{\min}$ come from the explicit form of the band structure.

We suggest that the transmission probability is given by the WKB approximation in the form [8]

$$D(\varepsilon) = \exp\left[-\frac{\zeta(\phi - \varepsilon)^{3/2} \upsilon(y)}{F}\right], \tag{10}$$

where $\zeta = 8\pi(2m)^{1/2}/3eh$, $y = (eF/4\pi\varepsilon_0)^{1/2}/\phi$, ϕ is the work function, ε_0 is the dielectric constant, m — the electron mass. The function $\upsilon(y)$ describes a deviation of the barrier from the triangle form due to image effects and can be approximated as $\upsilon(y) \approx 1 - y^{1.69}$ (see [25]).

4. RESULTS

The FEC and the FEED ($P(\varepsilon)$) are connected by (see, e.g., [8])

$$j^{\rm out} = \int\limits_{-\infty}^{\infty} d\varepsilon P(\varepsilon). \tag{11}$$

The explicit form of $P(\varepsilon)$ for few-layer graphene can be found from (9). Indeed, for layers of a large (infinite) size the sum in (9) can be replaced by the integral and, correspondingly, one has to use $\varepsilon_{\min}(p_y)$ and $\varepsilon_{\max}(p_y)$ instead of $\varepsilon^q_{\min}$ and $\varepsilon^q_{\max}$. In our case, these p_y-dependent functions can be easily calculated from (5). Finally, we have to change the order of integration in (9).

The result for ABA-type multilayers is

$$P(\varepsilon) = \frac{2g}{\upsilon_F} f(\varepsilon) D(\varepsilon) \sum_{n=1}^{n=N} \theta(\epsilon_n) \sqrt{|\varepsilon| \epsilon_n}, \tag{12}$$

where $\epsilon_n = |\varepsilon| + \gamma_1^n$, $g = 4e/(h^2 Nc)$, and $\theta(\epsilon)$ is the Heaviside step function. FEEDs for three- and four-layered Bernal stacking graphene are shown in Fig. 3, *a* and *b*. The results for ABC-type stacking have a very cumbersome form and, therefore, we present only the final curves in Fig. 3, *c* and *d*. One can see that both the heights and the positions of subpeaks for AB and ABC multilayers differ.

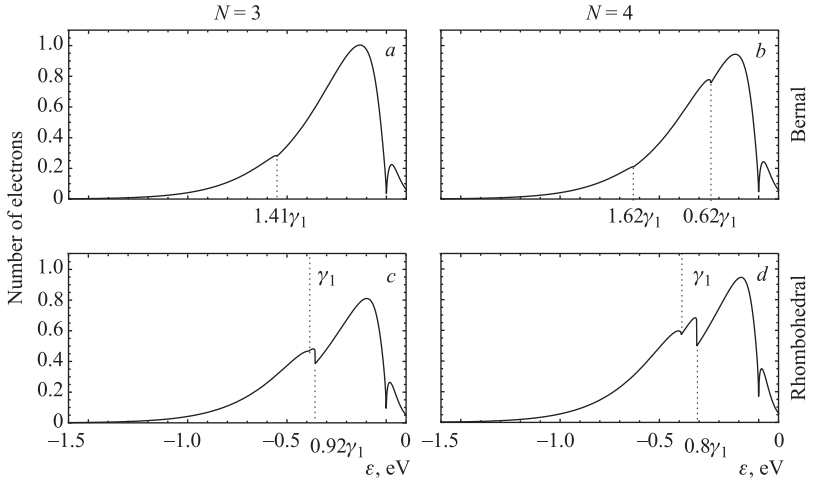

Fig. 3. Reduced FEED for three- to four-layer graphene of AB and ABC type. All SWMcC parameters except for γ_0 and γ_1 are put to be zero, $F = 4$ V/nm, $T = 300$ K. The peak height for Bernal stack with $N = 3$ is chosen to be unity. The positions of the distinctive points are indicated

CONCLUSION

In conclusion, we have calculated the FEED for few-layer graphene films and found the presence of characteristic subpeaks originated from involving in the emission process of additional branches in the energy spectrum of layered structures. Since the peak positions are directly determined by the number of layers, the discovery of such peaks in the FEED would be a clear manifestation of the quantum size effect. Therefore, the experimental studies of the FEED for CNSs are very relevant. Furthermore, the FEED analysis gives a new experimental tool to estimate the interlayer interaction constants (along with Raman scattering in [26] and photoemission methods in [27]) and provides important information on the concrete types of emitting CNSs. Moreover, it allows one to identify not only the number of layers but also the type of stacking in emitting CNSs.

This work has been supported by the Russian Foundation for Basic Research under grant No. 08-02-01027.

REFERENCES

1. *Wang J. J. et al.* // Appl. Phys. Lett. 2004. V. 85. P. 1265.
2. *Wang J. J. et al.* // Carbon. 2004. V. 42. P. 2867.
3. *Bagge-Hansen M. et al.* // J. Appl. Phys. 2008. V. 103. P. 014311.
4. *Kun Hou et al.* // Appl. Phys. Lett. 2008. V. 92. P. 133112.
5. *Goki Eda et al.* // Ibid. V. 93. P. 233502.
6. *Malesevic A. et al.* // J. Appl. Phys. 2008. V. 104. P. 084301.
7. *Lipson H., Stokes A. R.* // Proc. Roy. Soc. A. 1942. V. 181. P. 101.
8. *Gadzuk J. W., Plummer E. W.* // Rev. Mod. Phys. 1973. V. 45. P. 487.
9. *Mayer A., Miskovsky N. M., Cutler P. H.* // J. Phys.: Condens. Matter. 2003. V. 15. P. R177.
10. *Stark D., Zwicknagl P.* // Appl. Phys. 1980. V. 21. P. 397406.
11. *Wysockia J. K., Stark D.* // Surf. Sci. 1991. V. 247. P. 402.
12. *Johnson S., Zülicke U., Markwitz A.* // J. Appl. Phys. 2007. V. 101. P. 123712.
13. *Liang S.-D. et al.* // Appl. Phys. Lett. 2004. V. 85. P. 813.
14. *Katkov V. L., Osipov V. A.* // JETP Lett. 2009. V. 90. P. 304.
15. *Katkov V. L., Osipov V. A.* // J. Phys.: Condens. Matter. 2008. V. 20. P. 035204.
16. *Latil S., Henrard L.* // Phys. Rev. Lett. 2006. V. 97. P. 036803.
17. *Partoens B., Peeters F. M.* // Phys. Rev. B. 2006. V. 74. P. 075404.
18. *Slonzewski J. C., Weiss P. R.* // Phys. Rev. B. 1958. V. 109. P. 272.

19. *McClure J. W.* // Phys. Rev. B. 1957. V. 108. P. 612.

20. *Dresselhaus M. S., Dresselhaus G.* // Adv. Phys. 1981. V. 30. P. 139.

21. *Mikitik G. P., Sharlai Yu. V.* // Phys. Rev. B. 2008. V. 77. P. 113407.

22. *McClure J. W.* // Carbon. 1969. V. 7. P. 425.

23. *Guinea F., Castro Neto A. H., Peres N. M. R.* // Phys. Rev. B. 2006. V. 73. P. 245426.

24. *Arovas D. P., Guinea F.* // Phys. Rev. B. 2008. V. 78. P. 245416.

25. *Hawkes P. W., Kasper E.* Principles of Electron Optic. V. 2. London: Acad. Press, 1989.

26. *Malard L. M. et al.* // Phys. Rev. B. 2007. V. 76. P. 201401(R).

27. *Ohta T. et al.* // Phys. Rev. Lett. 2007. V. 98. P. 206802.